Chemistry—Methods

Review
doi.org/10.1002/cmtd.202200067

Chemistry Europe
European Chemical Societies Publishing

www.chemistrymethods.org

Methods to Characterise Enzyme Kinetics with Biological and Medicinal Substrates: The Case of Alkaline Phosphatase

Scott G. Harroun*[a, b] and Alexis Vallée-Bélisle*[b, c]

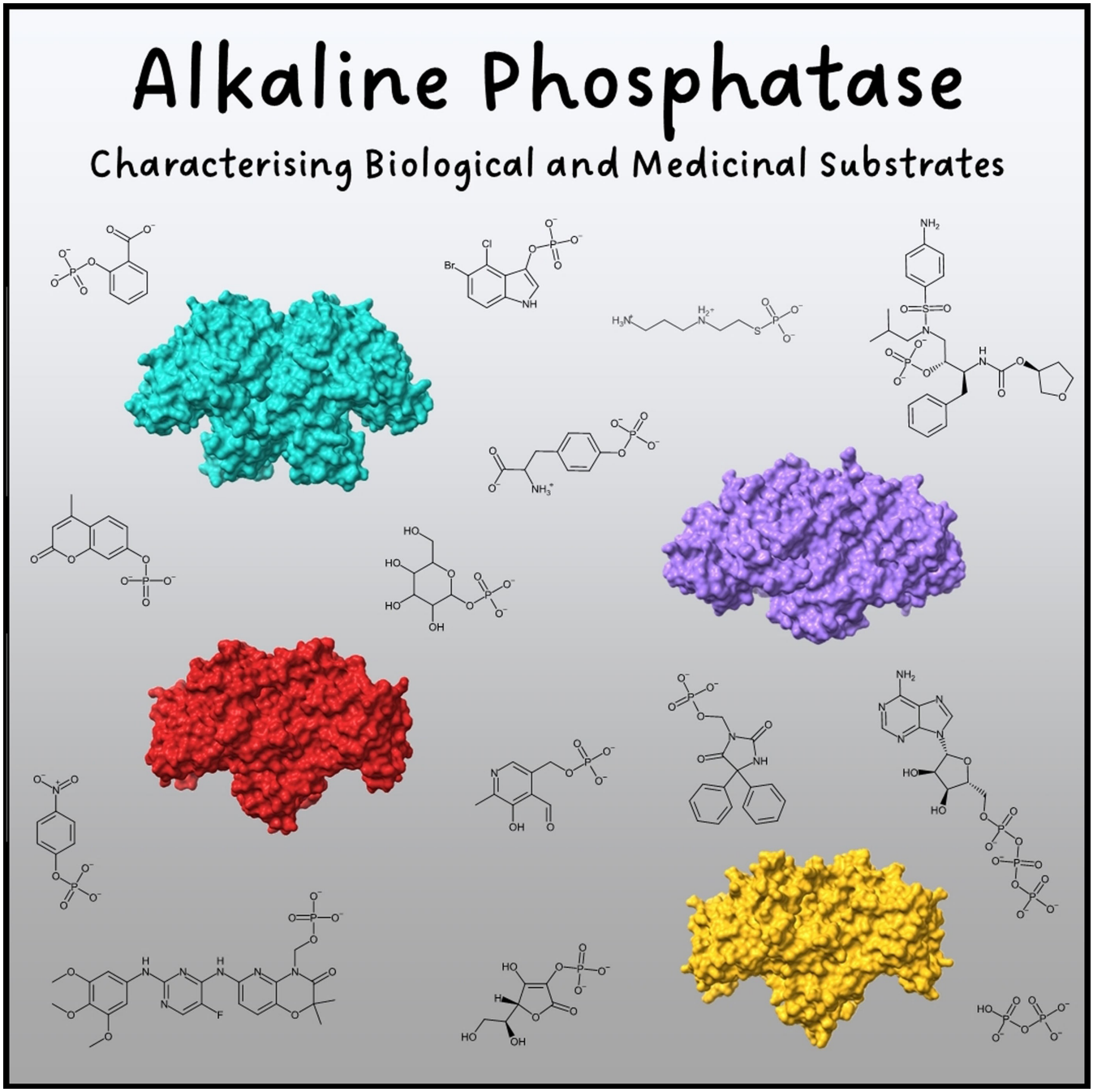

Alkaline phosphatase (AP) enzymes are of broad interest in fields ranging from biochemistry and medicine to biotechnology and nanotechnology. Characterising the catalytic activity of AP is typically realised by either employing non-natural signal-generating substrates that are detectable by absorbance and fluorescence spectroscopy or by quantifying the release of inorganic phosphate by the classic malachite green assay. The latter method is often required for studying "spectroscopically silent" biomolecular substrates, but it does not enable continuous monitoring of kinetics in real-time. In recent years, newer techniques for studying AP function have been developed to circumvent this limitation, including fluorescent and colourimetric substrate-specific assays based on supramolecular chemistry, organic probes and nanomaterials, as well as other assays based on isothermal titration calorimetry, direct detection with infrared spectroscopy and mass spectrometry, and monitoring conformational change by fluorescent nanoantennas. Here, we review these strategies and comment on their strengths and weaknesses in the context of AP.

1. Introduction

Enzymes and the reactions that they catalyse are critical to a wide range of fields. Beyond their important functions in biology, domains such as organic synthesis,[1] nanotechnology,[2] medicine,[3] and industries including food and biofuel production[4] are just a few of the many applications that utilise enzymes. Among the various types of enzymes, the alkaline phosphatase family (AP; EC 3.1.3.1) has attracted enormous research interest.[5] Indeed, much has been written about APs, as evidenced by a search on PubMed for "alkaline phosphatase" returning over 100,000 results! Investigation of this enzyme ranges from employing microbial APs in industrial biotechnology,[6] to exploring its biological role in animals,[7] and studying human APs for health applications.[8] Substantial efforts have been devoted to characterising the four isozymes of AP present in humans: intestinal alkaline phosphatase (IAP), placental alkaline phosphatase (PLAP), placental-like or germ cell alkaline phosphatase (GCAP), and tissue-nonspecific alkaline phosphatase (TNAP) found throughout the body but mainly in the liver, kidney, and bones.[9] These and other APs have a conserved active site that can dephosphorylate phosphate monoesters and other phosphate-containing substrate molecules to yield inorganic phosphate (P_i) and an alcohol or a phenol.

The substrates transformed by APs are of immense interest (Figure 1). However, our knowledge of the natural substrates of APs is mainly limited to TNAP and IAP.[10] For example, TNAP splits pyrophosphate (PP_i) to form two molecules of P_i. Since PP_i is an inhibitor of bone mineralisation, TNAP deficiency caused by genetic mutations can thus result in hypophosphatasia of bones/teeth and elevated levels of PP_i in plasma and urine.[11] TNAP also converts pyridoxal 5′-phosphate (PLP), the active form of Vitamin B_6 and a vital coenzyme, to pyridoxal to enable its diffusion across cellular membranes. After this, it can be phosphorylated once again. An absence of TNAP in the brain can impede neurotransmitter synthesis, thereby causing epileptic seizures in infants with hypophosphatasia.[12] Phosphoethanolamine (PEA) is also a putative natural substrate of TNAP, but its purpose remains unknown.[12a] Recently, phosphocholine has been proposed too as a natural substrate of liver TNAP.[13] In addition to these small molecules, phosphorylated osteopontin protein has been recognised as a substrate of TNAP in the context of mineralisation.[12] Intestinal AP is likewise of considerable biomedical interest.[14] Via dephosphorylation, IAP re-

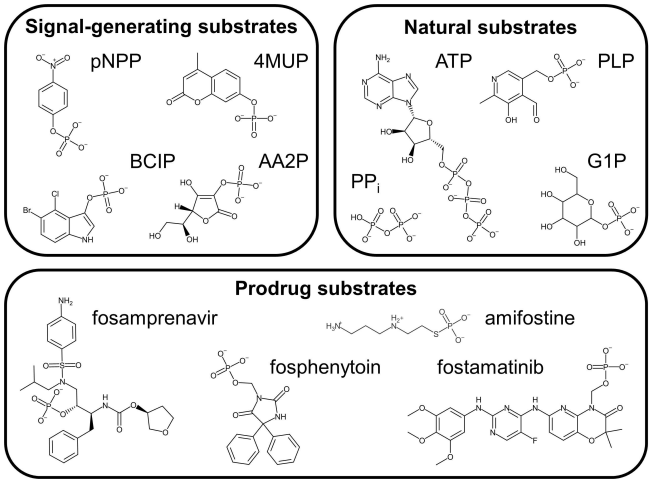

Figure 1. Chemical structures of various alkaline phosphatase substrates. Signal-generating substrates include pNPP, used for UV-Vis spectroscopy; 4MUP, used for fluorescence spectroscopy; BCIP, used for surface-enhanced Raman spectroscopy; and AA2P, used for electrochemical assays. Note that some substrates can be employed with more than one type of instrumentation. Natural substrates (also called physiological substrates or *in vivo* substrates) include ATP, which is hydrolysed by IAP; and PLP and PP_i, which are hydrolysed by TNAP. Some microbial APs can hydrolyse G1P. Prodrug substrates converted to their active metabolite forms by APs include fosamprenavir, used for HIV infection; fosphenytoin, used for convulsive status epilepticus; amifostine, used in cancer chemotherapy and radiotherapy; and fostamatinib, for chronic adult immune thrombocytopenia.

[a] *Dr. S. G. Harroun*
Département de génie physique
Polytechnique Montréal
Montréal, Québec H3C 3A7 (Canada)
E-mail: sg.harroun@polymtl.ca

[b] *Dr. S. G. Harroun, Prof. Dr. A. Vallée-Bélisle*
Département de chimie
Université de Montréal
Montréal, Québec H3C 3J7 (Canada)

[c] *Prof. Dr. A. Vallée-Bélisle*
Département de biochimie et médecine moléculaire
Université de Montréal
Montréal, Québec H3C 3J7 (Canada)
E-mail: a.vallee-belisle@umontreal.ca

duces the toxicity of lipopolysaccharide (LPS) released by the Gram-negative bacteria in the intestines. Another function of IAP is to hydrolyse luminal phosphates such as adenosine triphosphate (ATP), adenosine diphosphate (ADP), and adenosine monophosphate (AMP) to adenosine. This function has known roles concerning bicarbonate secretion, regulating duodenum surface pH, and promoting the growth of the intestinal commensal microbiota.[14a–c] Human APs are also leveraged to convert various prodrugs to their active metabolite forms.[15] Finally, APs from non-mammalian species likewise comprise an active area of research, including elucidating their natural substrates and use thereof as sources of phosphate.[16]

The case is strong for the importance of having methods to characterise the enzymatic activity of APs (Figure 2a). However, many biological/medicinal substrates and their products are difficult to detect. This situation has necessitated using either signal-generating substrates to yield a product that can be monitored by various analytical techniques (Figure 2b) or detecting released phosphate (Figure 2c). However, these methods are unsuitable for many applications since signal-generating substrates are not found in nature, while methods based on phosphate quantification do not enable rapid and continuous assays. This inadequacy has prompted the development of alternative approaches. Many strategies developed in response to this need are based on detecting a non-phosphate product by its specific interaction with a recognition element to induce a signal change. Alternatively, the substrate can be detected in a similar manner (Figure 2d). Other works have demonstrated the direct detection of product molecules (Figure 2e) or detection based on thermodynamics (Figure 2f). And in our work, we have recently reported a novel method based on detecting conformational change (Figure 2g). Here, we review recent advances concerning methods for characterising the enzymatic activity of AP with an emphasis on "spectroscopically silent" substrates. Rather than detecting the presence of AP,[17] many of these methods can be used to derive Michaelis–Menten kinetic parameters (i.e., Michaelis constant, K_M; catalytic rate constant, k_{cat}; and catalytic efficiency, k_{cat}/K_M). We hope this review will be informative for researchers eager to study reactions mediated by this important enzyme. Moreover, many of the principles discussed herein should also apply to other enzyme-substrate systems if the protocols are modified accordingly.

2. Detection Methods

2.1. Detecting non-phosphate products from signal-generating substrates

The first category of methods involves substrates that, upon conversion by AP, generate a product with an easily detectable signal (Figure 2b). A classic and widely employed chromogenic substrate is *p*-nitrophenylphosphate (pNPP), which AP converts to P_i and yellow *p*-nitrophenol (pNP).[18] Ultraviolet-visible (UV-Vis) absorbance spectroscopy can monitor this reaction in real-time. For example, pNPP was recently employed in a study of the pH-dependent binding of chloride ions to a marine bacterial AP from *Vibrio splendidus*.[19] Analogues of pNPP that release the same pNP product can be employed to characterise other activities of APs (e.g., diesterase, triesterase, and sulfatase).[20] Similarly to pNPP, AP converts 4-methylumbelliferylphosphate (4MUP) to P_i and fluorescent 4-methylumbelliferone (4MU).[21] Fluorescence spectroscopy can monitor this reaction in real-time. 4MUP was recently used to discriminate isozymes of AP at the single-molecule level.[22] ELF-97 is another popular fluorogenic substrate.[23] These substrates are commercially available and widely used.[24]

New fluorogenic substrates of AP have been introduced. These substrates often provide advantages in complex environments such as serum, cells, and tissues. Examples include aggregation-induced emission (AIE),[25] ratiometric substrate and

Scott G. Harroun is a Postdoctoral Fellow in Engineering Physics in the research group of Michel Meunier at Polytechnique Montréal. He obtained his PhD in Chemistry under the supervision of Alexis Vallée-Bélisle at Université de Montréal, where he developed fluorescent nanoantennas to monitor the conformational changes of proteins. Before that, he worked as a researcher at National Taiwan University after earning his MSc and BSc degrees at Saint Mary's University. He currently holds a Banting Postdoctoral Fellowship (2022) in support of his research. His research interests include DNA nanotechnology, protein biosensors, plasmonic nanoparticles, and surface-enhanced Raman spectroscopy.

Alexis Vallée-Bélisle is an Associate Professor of Chemistry at Université de Montréal (UdeM) and Canada Research Chair Tier II in Bioengineering and Bionanotechnology. He obtained his PhD in Biochemistry in 2008 under the supervision of Steven Michnick at UdeM. He realised his postdoctoral studies in Bioengineering with Kevin Plaxco at UC Santa Barbara (2008–2012). Prof. Vallée-Bélisle's laboratory develops bio-inspired nanotechnologies for both fundamental and health applications. His contributions have been recognised by an FRQ Santé Early Career fellowship, a Canada Rising Star in Global Health prize (2013), a UdeM Rector's Award (2018), the Effervescent Star Award from Montreal In Vivo (2019), and the e-Health Solution Award from the Quebec Ministry of Health and Social Services (2019). Prof. Vallée-Bélisle co-founded Anasens Diagnostics, a Montreal- and Boston-based company that develops digital home diagnostic tests for blood and saliva molecular analysis.

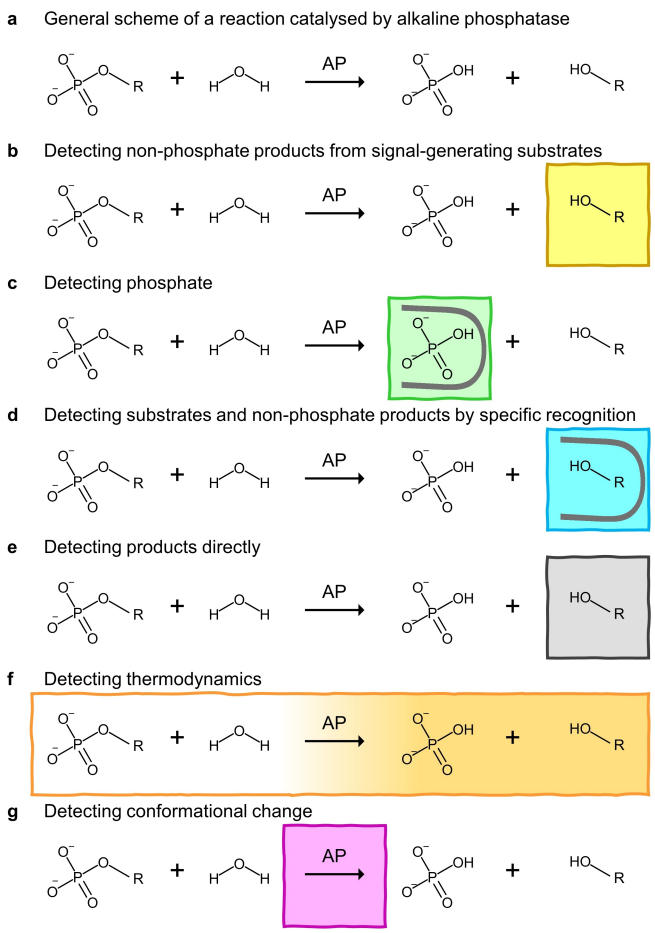

Figure 2. Categories of methods to monitor alkaline phosphates kinetics. (a) General reaction scheme of phosphomonoesterase reaction catalysed by AP. (b) The hydrolysis of signal-generating substrates like pNPP, for example, can be detected via its yellow product pNP by employing UV-Vis spectroscopy. (c) The phosphate released from the substrate can be detected by phosphate quantification, such as the classic malachite green assay. (d) The specific recognition of non-phosphate products can be detected by UV-Vis and fluorescence spectroscopies with various recognition elements such as supramolecular chemosensors, gold nanoparticles, organic probes, DNA aptamers, etc. Alternatively, the substrate can be detected. (e) The products can also be monitored directly by IR spectroscopy, ^{31}P NMR spectroscopy, and MS-based methods. (f) The thermodynamics of the reaction can be detected by isothermal titration calorimetry to characterise the reaction. (g) The conformational changes of AP during the reaction can be followed by employing fluorescent nanoantennas to derive the kinetic parameters. Generally speaking, in (b, d), the substrate's –R group is particular to the assay, whereas in (c, e, f, g), a substrate with any –R group can be monitored.

product emission,[26] emissions at longer wavelengths, including in the near-infrared (NIR) range,[27] insoluble products to prevent diffusion from the inside of cells,[28] and fluorescent phosphopeptides that undergo enzyme-catalysed self-assembly that can be employed to study cellular uptake.[29] Some fluorogenic substrates are reported to display specific recognition by AP, and which are not hydrolysed by other phosphatases.[30] Substrates have also been designed for multiplexed single-molecule analysis.[31] Of course, substrates for use with other approaches are available too. These include bioluminescence,[32] electrochemistry,[33] UV-Vis spectroscopy,[34] Raman spectroscopy and surface-enhanced (resonance) Raman spectroscopy (SERS and SERRS),[35] chemical exchange saturation transfer magnetic resonance imaging (CEST MRI),[36] electron paramagnetic resonance (EPR) spectroscopy,[37] and ^{19}F nuclear magnetic resonance (NMR) spectroscopy.[38]

Although many options are available, a limitation shared by these methods is their reliance on the inherent properties of a particular substrate or its product to generate a signal change depending on the instrument being used to follow the reaction. This limitation renders these otherwise useful methods unsuitable for the general characterisation of the natural and medicinal substrates of AP. Moreover, kinetic parameters could differ between these signal-generating substrates and their natural counterparts.

In some of the examples mentioned above, the substrate or its product does happen to be a bioactive molecule, but each method still remains limited to specific substrates. For example, AP can convert fosfosal, an analgesic and nonsteroidal anti-inflammatory drug (NSAID), to salicylic acid that is found in the sap of willow trees (Figure 3a).[15f] This enzymatic reaction can be characterised by CEST MRI via the chemical shift due to the exchangeable proton of the product (Figure 3b).[36] Alternatively, this enzymatic reaction can be detected by Raman spectroscopy due to the higher signal intensity of salicylic acid and its distinct vibrational fingerprint. Reaction kinetics can be followed via the Raman band observed at 1326 cm^{-1} (Figure 3c).[35c] Nevertheless, swapping fosfosal for another biomolecular substrate would not necessarily provide a signal change readily detectable by CEST MRI or Raman spectroscopy. Equally, other instruments may not readily detect the conversion of fosfosal to salicylic acid. As another example, the AP-catalysed conversion of ascorbic acid 2-phosphate (AA2P) to ascorbic acid (Vitamin C) can be characterised by cyclic voltammetry (CV), but this electrochemical method would not necessarily work for other substrates, nor would AA2P necessarily work for other non-electrochemical methods.[39] As a final example, the product of 4MUP is of biomedical interest (Note, 4MU is also called hymecromone),[40] but that does not necessitate that all AP-activated prodrugs could yield a product molecule with an easily detectable fluorescent signal. Nearly all AP substrates, however, do have one component in common – their phosphate group(s). Universal methods based on the detection of P_i are the focus of the next section.

2.2. Detecting phosphate

The second category of methods involves detecting the P_i product (Figure 2c). Although APs can also display sulfatase activity, for example,[20,41] the detection of phosphatase activity is relevant for most kinetic studies of this enzyme. Detection of P_i is necessitated by the fact that, unlike what occurs for signal-generating substrates, the non-phosphate products of biological and medicinal substrates typically do not provide a useful signal for many analytical techniques.

One can detect the released P_i by reaction with molybdate in strong acid to yield 12-molybdophosphoric acid (12-MPA).[42]

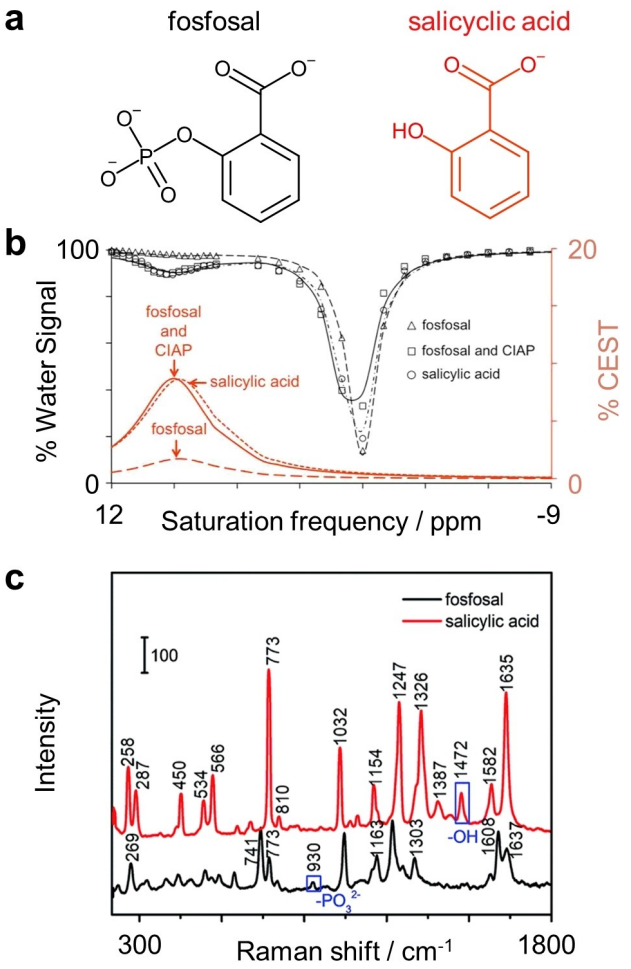

Figure 3. Signal-generating AP substrates. (a) Molecular structures of fosfosal (substrate) and salicylic acid (product). (b) Different signals are obtained for fosfosal and salicylic acid via CEST MRI. Adapted with permission from Ref. [36]. Copyright 2016 American Chemical Society. (c) Likewise, different signals are obtained for fosfosal and salicylic acid via Raman spectroscopy. Adapted with permission from Ref. [35c]. Copyright 2019, Royal Society of Chemistry.

It can then be quantified by three categories of methods, as noted elsewhere.[43] The first method involves prior labelling of the phosphate moiety with ^{32}P. The complex can be extracted in an organic water-immiscible solvent, and then one can measure its radioactive emission. While highly sensitive, this method requires complicated synthesis and procedures. The second method, the molybdenum blue reaction, involves reducing 12-MPA to enable colourimetric detection.[44] Finally, the third and more sensitive method involves the reaction of 12-MPA with a dye, such as malachite green.[106] A surfactant must be added due to the insolubility of the complex. Moreover, the low stability of the dye necessitates its preparation on the same day.[45] Recent adaptations[43,46] of the malachite green assay have been introduced that overcome some limitations. For example, one provides long-term storage stability.[43] Overall, procedures for quantifying P_i have the benefit of being effectively universal. Still, they are also laborious and do not enable data collection in real-time, also known as a continuous assay. Even so, the malachite green assay continues to be widely employed, including in prominent studies.[14d]

Some P_i quantification methods do provide a continuous assay, but they are unsuitable for AP, such as the EnzChek phosphate assay.[47] Therein, the released P_i and 2-amino-6-mercapto-7-methylpurine riboside are converted by purine nucleoside phosphorylase to ribose 1-phosphate and 2-amino-6-mercapto-7-methylpurine. One follows the reaction with UV-Vis spectroscopy via the shift from 330 nm to 360 nm. This assay is suitable for ATPases, but APs would also hydrolyse the ribose 1-phosphate, thereby affecting the observed kinetics.

"Phosphate mop" methods have also been demonstrated for real-time monitoring of phosphatase activity. One approach monitors the P_i product via a phosphate-binding protein labelled with a fluorophore.[48] In the context of AP, however, the released P_i is not simply a product but also a competitive inhibitor. While avoiding the inhibitory effects of P_i may be desirable in some applications, such as enzyme-linked immunosorbent assays (ELISAs),[49] kinetic characterisations with sequestered P_i could, in principle, deviate relative to biological conditions wherein some inhibition via the released phosphate would occur. A similar argument concerning the deviation of kinetic parameters would apply to a method based on transforming a weakly fluorescent complex of Eu^{3+} and tetracycline that coordinates P_i and enhances the fluorescence.[50] It could also apply to Ce^{3+}-induced quenching of graphene quantum dots (GQDs) or other materials for which competitive formation of $CePO_4$ recovers the fluorescence,[51] and another method based on Tb^{3+} ions with luminescent zinc metal–organic frameworks (Tb@Zn-MOFs).[52] Therefore, P_i sequestration in continuous assays ought to be useful for detecting the presence of AP via its activity, as proposed in the above studies, but not for the derivation of kinetic parameters. Next, instead of assays that target P_i, we will evaluate those based on specific recognition of the other non-phosphate product molecule released from a substrate. Importantly, these product molecules are not inhibitors of AP, so their sequestration should not affect the kinetic parameters.

2.3. Detecting substrates and non-phosphate products by specific recognition

The third category of methods detect either the reaction of one particular substrate, such as PP_i or ATP, or a class of substrates. These involve the indirect detection of the non-P_i product or the initial substrate via specific interaction with a recognition element to mediate a signal change (Figure 2d).

First, we will consider fluorescent assays for PP_i. A prominent example to detect PP_i hydrolysis employs a fluorescent poly(phenylene ethynylene) polymer ($PPECO_2$) that is first quenched by cupric ions. The addition of PP_i increases fluorescence due to complexation with the ions. Thus, when the subsequent addition of AP catalyses the hydrolysis of PP_i to $2P_i$, one can monitor the enzyme's activity by a decrease of fluorescence as the cupric ions rebind to the polymer. This approach can also characterise the P_i product's inhibition

constant (K_i).[53] Although this study was demonstrated with bovine IAP, there is no reason to believe the assay would not work for TNAP, which is more relevant for the PP_i substrate. A more recent study synthesised a benzimidazole-based zinc complex, which was selective for PP_i that enhances its fluorescence. Then, AP activity toward PP_i could be monitored via a decrease in fluorescence.[54] Another study reported a sensing strategy with fluorescent carbon quantum dots (CQDs). Although this assay was employed to quantify AP, it could potentially be applied to characterise enzyme-substrate kinetics.[55]

Fluorescent assays are available for the adenosine series of AP substrates. In one case, a fluorescent perylene probe was designed to be quenched upon binding of ATP, but the fluorescence recovers after hydrolysis of the ATP substrate by calf intestinal alkaline phosphatase (CIAP). ADP and AMP could also quench the fluorescence, although to a lesser extent than ATP, whereas adenosine and PP_i did not affect the signal. The oxyanion vanadate, a competitive inhibitor, was characterised as well.[56] A recent study reported three phenanthroline-based zinc complexes that display a decrease in fluorescence upon binding of ATP. A small signal change also occurred upon introduction of ADP, but the effect was negligible for other molecules, including other nucleotide triphosphates. Real-time monitoring of AP activity was reported, but it is unclear if this method could also be employed to determine Michaelis–Menten kinetic parameters.[57] In another study demonstrated with CIAP and porcine kidney AP, a structure-switching DNA aptamer was employed to detect enzymatic activity. The signal change was provided by labelling the aptamer with a fluorophore and quencher pair. It was most sensitive to AMP but also could detect the hydrolysis of ADP and ATP, and characterise the effect of the inhibitor levamisole.[58]

Colourimetric nanoparticle assays are also available for various substrates. Conversion of ATP to adenosine results in the aggregation of gold nanoparticles (Au NPs) and a colour change from red to blue. Although kinetic parameters were not reported, the colour change was time-dependent, and therefore, the assay could plausibly be adapted to study kinetics. Note that non-specific interaction in complex media causing aggregation of Au NPs must also be considered.[59] A more recently reported colourimetric method is based on converting cysteamine S-phosphate to cysteamine (Figure 4a). This product molecule, a thiol that is reactive toward gold, aggregates Au NPs functionalised with Zonyl FSN-100 (FSN-AuNPs) and shifts the colour from red to purple (Figure 4b). Kinetic parameters were reported for cysteamine S-phosphate. Presumably, this method could also work for other substrates that release a thiol product, such as amifostine. The authors demonstrated that non-thiol substrates or their products, such as AMP, ADP, and ATP, did not give rise to a signal change.[60] Another study leveraged histidine-protected gold nanoclusters that display peroxidase-like activity, thereby mediating chromogenic detection of colourless 3,3′,5,5′-tetramethylbenzidine (TMB) being converted to its blue oxidised form. This process, however, can be blocked by molecules that contain a pyrophosphate moiety. Accordingly, this method can detect ATP, ADP, and PP_i, but

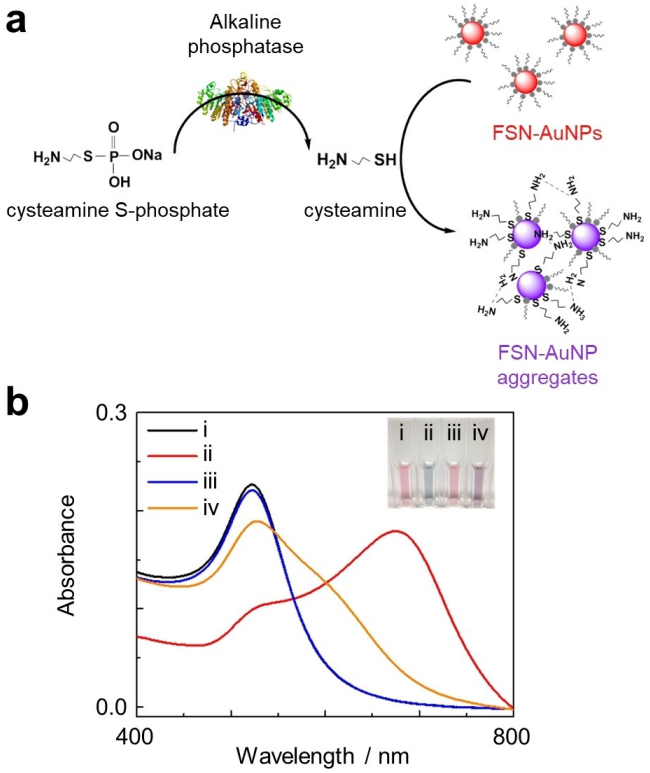

Figure 4. (a) Gold nanoparticle aggregation assay with AP and the substrate cysteamine S-phosphate. (b) UV-Vis absorption spectra of (i) FSN-AuNPs, (ii) FSN-AuNPs + cysteamine, (iii) FSN-AuNPs + cysteamine S-phosphate, and (iv) FSN-AuNPs + cysteamine S-phosphate + AP. The inset shows photographs of the colour changes. Reprinted from Ref. [60], Copyright 2020, with permission from Elsevier.

AMP had a negligible effect on the signal, as did adenosine and P_i. This method can detect AP activity with pyrophosphate-containing substrates, but whether it could be applied to characterise kinetic parameters remains unclear.[61]

Inspired by indicator displacement assays (IDA) based on competitive binding titration, supramolecular tandem assays have been developed to monitor enzyme activity.[62] This method employs a reporter pair consisting of a macrocyclic "host" molecule and a fluorescent dye "guest" molecule (Figure 5a). In the product-selective design, the macrocycle binds the substrate weakly and the product strongly. By enabling competition via their differential binding affinities, the substrate will not displace the fluorescent dye from the macrocycle, but the product will. This order of selectivity is reversed in the substrate-selective design. Depending on the dye's photophysical properties and the chemical environment, the fluorescence may be higher or lower while complexed with the macrocycle, but in either case, the reaction can be continuously monitored by the change in fluorescence signal intensity.[62–63] A recent study demonstrated supramolecular tandem enzyme assays to monitor kinase and phosphatase activity. For the latter, it employed a reporter pair consisting of the macrocycle cucurbit[7]uril (CB7) and the fluorescent dye berberine (Figure 5a). This pair could continuously monitor the AP-mediated hydrolysis of phosphotyrosine (PTyr; also called O-phospho-L-

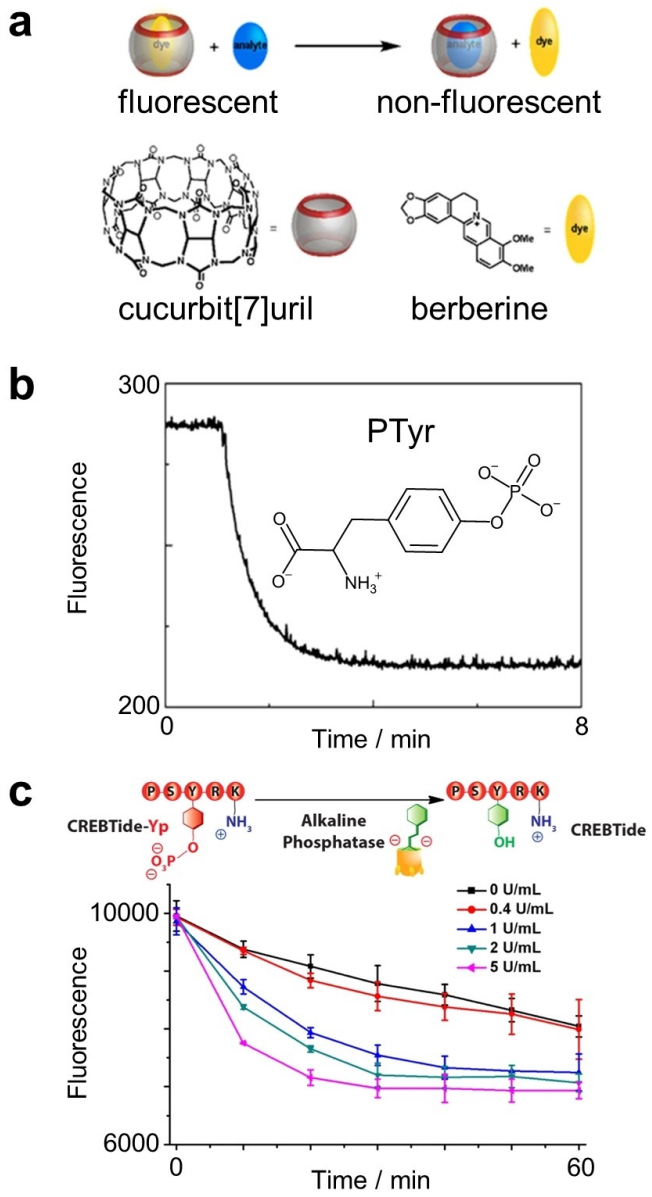

Figure 5. Chemosensor methods to monitor AP substrates. (a) Principle of supramolecular tandem enzyme assay for AP substrate PTyr and (b) its application for continuous monitoring of this reaction. Adapted from Ref. [64] according to CC BY-NC 4.0, Copyright 2019, Liu et al. and published by Wiley-VCH. (c) Principle and assay of AP activity for a phosphorylated peptide (CREBtide-Yp). Adapted with permission from Ref. [65]. Copyright 2018 American Chemical Society.

tyrosine) (Figure 5b).[64] Detection of PTyr is noteworthy because phosphorylated peptides and amino acids could serve as models of phosphoprotein substrates. Other recent studies have reported supramolecular tandem enzyme assays using various host–guest combinations to monitor AP with relevant biomolecular substrates. These include monitoring ATP with the pair calixpyridinium and 1,3,6,8-pyrenetetrasulfonic acid tetrasodium salt (PyTS),[66] as well as PLP with guanidinocalix[5]arene and fluorescein.[67] Another study further revealed that it is possible to study AP with phosphorylated peptide substrates via a host–guest pair (Figure 5c).[65] Interestingly, this paper demonstrated that the host–guest concept could discriminate different peptides phosphorylated by protein kinase A. More specifically, the host–guest sensor with an array of metal ions provided differential responses to two peptides that undergo phosphorylation at distinct positions. Speculatively, an analogous strategy for AP activity toward phosphorylated peptide substrates might also be possible.

In consideration of the delicate balance of the affinities of the substrate, the product, and the fluorescent dye toward the host, an alternative chemosensor design is based on the associative binding assay (ABA).[68] In an example with the host cucurbit[8]uril (CB8) and fluorescent 2,7-dimethyldiazapyrenium (MDAP), the latter is not displaced from the macrocycle, but instead, the strategy relies on the differential affinities of an aryl substrate and its product for the host–guest complex. Substrate or product binding near the dye will, in turn, quench or enhance the fluorescence.[69] This strategy was demonstrated for real-time monitoring of the function of 12 enzymes, including AP from bovine intestinal mucosa. Hydrolysis of phenyl phosphate and 2-naphthyl phosphate (2-NP) quenched the fluorescence by binding their respective aryl products.[69] This strategy was subsequently employed in the context of membrane translocation to monitor membrane-impermeable 2-NP and its AP-mediated conversion to the permeable product.[70] Separately, binding to CB8 can also enhance the signal of the AP-generated product of the commercially available chemiluminescent substrate CDP-Star.[71]

Substrate-specific methods to characterise AP activity can provide a straightforward continuous assay for spectroscopically silent biomolecular and medicinal substrates. However, comparisons with classic assays[43–45] are often not included in studies reporting new probes to determine Michaelis–Menten kinetic parameters. While likely less of a problem for methods based on detecting non-P_i products, such omissions are concerning in methods based on the interaction of substrate molecules with recognition element molecules, which could potentially impact the observed kinetics. Aside from this consideration, the main limitation is that an assay for a substrate of interest may not be available in all cases. Moreover, for researchers interested in studying more than one substrate with AP, it is impractical to combine multiple different assays. Supramolecular chemosensor assays based on host–guest pairs offer more flexibility for studying APs with diverse substrates. However, a limitation of supramolecular tandem enzyme assays is finding the right balance of affinities for the substrate, the product, and the fluorescent dye with the macrocycle host. Associative binding assays developed in response have only been employed for non-natural AP substrates like 2-NP. Thus, while in principle the chemosensor strategy could potentially be universal if enough host–guest pairs are developed; in practice, it may instead represent a midpoint between purely substrate-specific AP assays on the one hand and generalisable assays for any substrate of AP on the other. Universal assays not based on the detection of P_i are the focus of the following three sections.

2.4. Detecting products directly

The fourth category of methods involves the direct detection of non-P_i products but without a component designed to provide a signal change (Figure 2e). P_i can often be detected too.

Following up on earlier work about ATP and P_i interaction with AP and the associated conformational changes,[72] infrared (IR) spectroscopy has been employed to follow AP activity toward natural substrates in cell studies. Reference IR spectra were first recorded for various substrates and P_i in a buffer solution. The substrates were pNPP, PP_i, AMP, ADP, ATP, uridine triphosphate (UTP), glucose-1-phosphate (G1P), and β-glycerophosphate (BGP). P_i exhibits two bands at 1076 and 990 cm^{-1} assigned to the asymmetric and the symmetric stretching vibrations of O–P–O, respectively. Due to the different chemical environments of unbound and bound phosphate, equivalent bands do not appear at the same positions in the spectra of the substrates. Thus, one can follow phosphatase activity by a change in the intensity of one or both bands (Figure 6). In the difference spectra, a spectrum measured at an indicated time minus the spectrum measured immediately after mixing the substrate, a decrease in band intensity corresponds to substrate consumption. In contrast, an increase in band intensity corresponds to the production of the P_i product. In this work, the specific activity was determined for the substrates, and the inhibitor levamisole confirmed the presence of TNAP. This method was demonstrated with human osteosarcoma Saos-2 cells, primary osteoblast cells from mice, and matrix vesicles from chicken embryo growth plates and epiphyseal cartilage.[73] In a subsequent study, the authors explored the use of two-dimensional correlation IR spectroscopy to resolve band overlap.[74] More recently, IR spectroscopy was employed in combination with ^{31}P NMR spectroscopy to monitor extracellular TNAP and other ectonucleoside triphoshatediphosphohydrolase sequential conversion of ATP to ADP and P_i, then to AMP and P_i, and finally adenosine and P_i, without the formation of PP_i during this process.[75] Overall, infrared spectroscopy provides time-dependent spectra by which one can follow enzyme kinetics.

Mass spectrometry can also be employed to study enzymatic reactions, including those of AP.[76] One study examined AP with ATP, ADP, and AMP via electrospray ionisation mass spectrometry (ESI-MS). The enzymatic reaction could be monitored in real-time until its completion after 30 min, albeit with a 3 min delay before the measurement could begin. The study noted how the classic malachite green spectrophotometric assay could not differentiate between P_i released from the initial substrate (ATP) and the intermediate products that are also substrates (ADP and AMP). In contrast, with ESI-MS, it was possible to directly observe ATP, ADP, AMP, and adenosine (Figure 7). This method enabled a comparison of the degradation rates of the three substrates at different pH values.[76b] However, Michaelis–Menten kinetic parameters were not reported with this technique. Elsewhere, conversion of prodrugs to their active form by AP has been studied by liquid chromatography-tandem mass spectrometry (LC–MS/MS).[77]

^{31}P NMR spectroscopy has been employed to study AP activity. For example, one study examined phosphorous compound use by *Chaetoceros tenuissimus* (a type of planktonic diatom). These included P_i, BGP as a phosphate monoester, and *sn*-glycero-3-phosphocholine as a phosphate diester.[78] Another

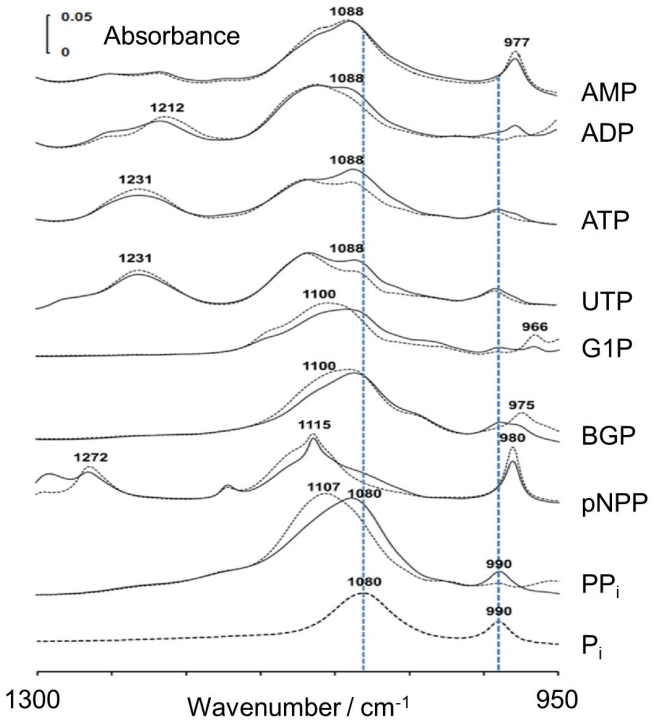

Figure 6. Monitoring AP activity with IR spectroscopy. Dashed lines are spectra recorded immediately after mixing substrates with Saos-2 cells, and solid lines are spectra recorded 30 min later. The dashed line at the bottom is the spectrum of the P_i product. Adapted from Ref. [73] according to CC BY 4.0., Copyright 2015, Ren et al. and published by PLOS.

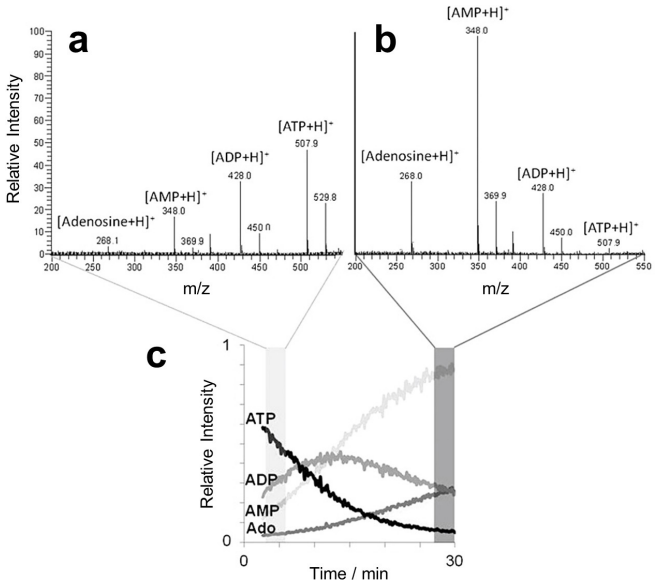

Figure 7. ESI-MS monitoring of AP kinetics. Assay component signal intensity average values at (a) 3–6 min immediately after the delay time and (b) after 27–30 min. In (c), the complete reaction kinetics are shown. Adapted with permission from Ref. [76b]. Copyright 2014, John Wiley & Sons, Inc.

recent study employed ^{31}P NMR spectroscopy to compare the degradation rates of phosphorous substrates by enzymes (AP and acid phosphatase) and naturally occurring oxide minerals (hematite, birnessite, and boehmite). The substrates were BGP, glucose-6-phosphate (G6P), diphosphopyridine nucleotide (also called α-nicotinamide adenine dinucleotide, α-NAD), AMP, ATP, phytic acid, and three polyphosphates.[79] Elsewhere, ^{31}P NMR spectroscopy was used to compare the hydrolysis rates of α-naphthyl phosphate (α-NP) and β-naphthyl phosphate (β-NP) due to the differential steric accessibility of the cleavable phosphate but otherwise similar properties. Thus, these two substrates served as a model of phosphorylated tyrosine versus serine and threonine residues in phosphoproteins and their hydrolysis by various phosphatase enzymes. In principle, this technique could also be utilised to study APs.[80]

Overall, IR spectroscopy and ^{31}P NMR spectroscopy can be used to follow AP activity in complex systems. MS-based methods can confirm the identity of product molecules, which is germane to the characterisation of prodrugs and intermediate substrates. However, for known enzyme-substrate systems focusing on kinetics, other less complicated methods may be desirable in some cases. In the following two sections, we will discuss other universal sensing strategies.

2.5. Detecting thermodynamics

The fifth category of methods involves detecting the thermodynamic parameters of the enzymatic reaction (Figure 2f). Isothermal titration calorimetry (ITC) has traditionally been employed to measure the thermodynamics of binding reactions, but it is emerging as a label-free method to monitor enzyme kinetics.[81] ITC measures the heat released or absorbed when one solution is titrated into another, such as one containing an enzyme and the other containing its substrate. This exothermic or endothermic heat change is converted to units of power based on the amount of electricity needed to maintain a constant temperature. It is plotted against time for each injection, thereby providing quantitative information about the thermodynamics of the reaction. ITC does not require signal-generating unnatural substrates, clear solutions for spectroscopy, coupled reactions for electrochemistry, and post-reaction processing of the sample.[81a]

Despite its advantages, one of the historical limitations in deriving enzymatic reaction kinetic parameters from ITC peaks had been that for short reactions taking place on the scale of seconds to tens of seconds, it was challenging to deconvolute the kinetics of the reaction from the kinetics of the instrument response. Thus, the experimental and calculated peaks for a single ITC reaction would differ, thereby hindering accurate extraction of kinetic information. Recent works have addressed the problems of ITC in the context of enzymatic reactions. One approach is based on multiple injections of varying concentrations of substrate. The authors employed a calibration method for the instrument and found that the initial rate of the ITC data corresponds to the reaction velocity. Thus, the method was called initial rate calorimetry (IrCal). This approach requires the determination of the enthalpy (ΔH) of the reaction, which is analogous to having to determine the molar extinction coefficient (ε) for kinetic characterisation by UV-Vis (e.g., pNPP). However, it differs because the substrate is not limited to those with favourable optical properties. The Michaelis–Menten kinetic parameters can then be determined with increasing substrate concentrations.[82] Another recent study employed a single injection strategy with a large substrate concentration. This work incorporated the post-reaction heat transfer and the electronic response of the instrument into a mathematical model to obtain an enzyme's kinetic parameters.[83] It could also be adapted to rapidly screen inhibitors in a single experiment.[84]

In the context of AP, the IrCal method was employed to characterise bovine intestinal AP with various substrates. With pNPP and 4MUP, the authors demonstrated that the kinetic values obtained with IrCal are consistent with those obtained by the classic spectroscopic methods. Then, it was shown that IrCal could characterise natural substrates, with ATP as an example. The method could also determine the K_i of the P_i product. Note that this study further investigated other enzymes besides AP.[82] A subsequent study addressed the applicability of ITC to high-throughput screening since chip-based calorimeters are more straightforward to automate than standard instruments. Chip-based calorimeters, however, suffer from incomplete mixing. Thus, this work introduced a calibration method and protocol to overcome this challenge. Similar kinetic parameters were obtained for pNPP via UV-Vis spectroscopy and the chip-based microfluidic calorimeter. Due to slow diffusion, the authors noted that the approach could not be employed for enzymes with a large substrate, such as a larger peptide or a protein. They also reported issues related to the lower volumetric heat generated in the microfluidic calorimeter than in standard isothermal titration calorimeters.[85] Nevertheless, ITC is a promising approach for the label-free characterisation of AP and other enzymes with biologically relevant substrates. The reader is advised to watch this exciting field. We will next consider another approach that, like ITC, had traditionally not been employed to study AP enzymes.

2.6. Detecting conformational change

The sixth and final category of methods involves detecting the conformational change of an enzyme while it is catalysing a reaction (Figure 2g). Using fluorophores to study the function of proteins is not new. Well-known examples are Förster resonance energy transfer (FRET)[86] and protein-induced fluorescence enhancement (PIFE).[87] Although dye labelling has been employed to study enzyme transient states[88] and dye-labelled linkers have been used in (bio)sensors,[89] no studies had used a linker to mediate dye-protein interactions that can be perturbed during protein function by small conformational changes. By employing DNA nanotechnology,[90] we explored this concept with AP. Our findings introduced fluorescent nanoantennas as a new strategy to characterise protein function via conformational change.[91] Though not intended to

be limited to one type of protein, our demonstration of this new biosensing strategy primarily focused on AP.

The assay is based on dye-protein interaction driven by a high local concentration. Small or large conformational changes will perturb this interaction, thereby providing a fluorescence signal change. This method can be used to monitor transient events, such as enzyme activity and thermal unfolding, as well as systems in equilibrium, such as inhibitor binding and protein-protein interaction. The assay's main component, a fluorescent nanoantenna, is made from a linker such as DNA or polyethylene glycol (PEG). It has a fluorescent dye at one end and an attachment moiety at the other (Figure 8a). For attachment, we typically used the convenience of biotin-streptavidin, although other strategies are also possible such as attaching thiolated nanoantennas to a protein's lysine residues. For simplicity, we focus here on biotin-streptavidin. One can connect biotin-labelled nanoantennas to biotin-labelled AP via the biotin-binding protein streptavidin. Concerning the dye, we found that fluorescein (FAM) was the best fluorophore to monitor the catalytic reaction of CIAP. And finally, concerning the linker, the sensitivity of this biosensor can be tuned by changing the nanoantenna's length and composition. We found that a 12-nucleotide single-stranded DNA (ssDNA) nanoantenna works best.

The nanoantenna-streptavidin-AP complex can characterise the enzyme's function by detecting conformational changes. The fluorescence signal obtained during substrate hydrolysis correlates with the presence of the transient enzyme-substrate complex. In our work,[91] fluorescent nanoantennas enabled the complete Michaelis–Menten kinetic characterisation of any substrate of AP in a "one-shot" measurement with the help of a fitting script.[84,91–92] We demonstrated this ability with 15 different substrates. These include natural substrates of intestinal AP and other mammalian APs, such as ATP, ADP, AMP, PP_i, and PLP, as well as other biomolecular substrates like BGP, guanosine triphosphate (GTP), phosphoenolpyruvate (PEP), phosphoserine (PSer), glucose-6-phosphate (G6P), fructose-6-phosphate (F6P), and phosphocreatine (PCr). Of note, we also characterised the kinetics of the prodrug amifostine. Shown here are three examples (Figure 8b). We further examined the effect of phosphate and various heavy metal competitive inhibitors, namely, molybdate, tungstate, vanadate, and arsenate, and characterised their effect on the AP-amifostine system. Finally, we demonstrated a plate reader assay with another protein system (i.e., Protein G and antibodies) to rapidly screen optimal nanoantennas and protein-protein interaction.[91]

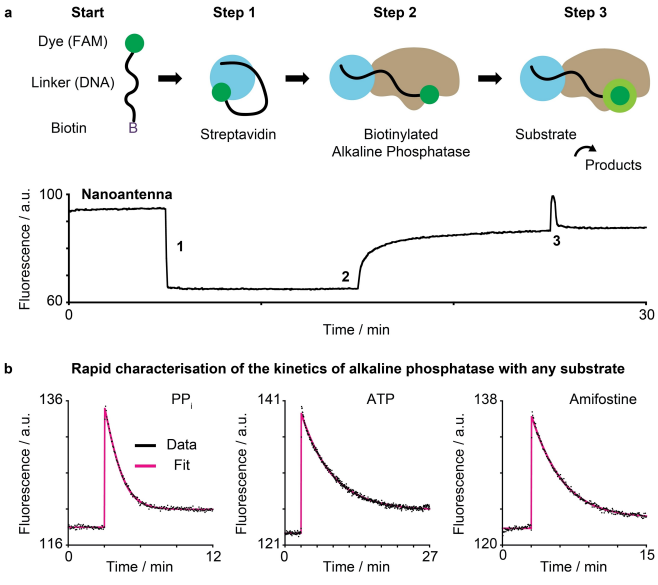

Figure 8. (a) Principle of fluorescent nanoantenna method with AP. Binding of the biotinylated fluorescent nanoantenna to streptavidin results in fluorescence quenching. Then, the binding of biotinylated AP results in a fluorescence increase. When a substrate is introduced, a transient "spike" in fluorescence is observed. (b) The Michaelis–Menten kinetic parameters can be extracted from the "spike" by employing a fitting script. Shown are PP_i, ATP, and amifostine. This figure is based on our previous work, Ref. [91] Copyright 2021, Harroun et al. and published by Springer Nature.

A potential limitation of fluorescent nanoantennas is the biotin-streptavidin attachment strategy. It is convenient for rapidly screening a protein of interest with many nanoantennas containing different dyes and linkers. Still, this approach is likely inapplicable for complex biological systems, such as studying APs in living organisms. It is also possible that biotinylating a protein could severely impact its function. However, as observed in our study and elsewhere, this was not the case for AP.[93] Nevertheless, we are exploring alternative attachment strategies. We also look forward to seeing how other researchers apply fluorescent nanoantennas for characterising APs and other proteins. Fluorescent nanoantennas may find applications in characterising various APs with biological substrates[16b,94] and inhibitors,[95] and to compare experimental results with data obtained *in silico*.[96]

3. Summary and Outlook

Many strategies are available to characterise AP-catalysed reactions. Classic and newer signal-generating substrates are often the easiest to detect. However, if one wishes to study this enzyme with "spectroscopically silent" substrates relevant to biology or medicine, quantifying released P_i had typically been required. In recent years, however, an expanded enzymology toolkit has emerged in the form of fluorescent and colourimetric substrate-specific assays, direct detection, isothermal titration calorimetry, and fluorescent nanoantennas. We have summarised the advantages and disadvantages of these various methods in Table 1.

When characterising an enzyme-substrate system, it is imperative to consider whether the enzyme and substrate concentrations are compatible with a particular assay and its limit of detection. Using the AP-ATP system as an example, the experimental conditions for various assays discussed herein are listed in Table 2. Although factors such as pH and enzyme source will affect the kinetics and thus optimal conditions, one could interpret that typical concentrations to study this enzyme-substrate system would be [AP] = ~1 to ~50 nM and [ATP] = ~1 to ~500 μM. This range of substrate concentrations

Table 1. Overview of methods to characterise alkaline phosphatase activity.

Category	Method	Continuous?	Any substrate?	Advantage	Disadvantage	Key References
Detecting signal-generating substrates	pNPP, 4MUP, BCIP, AA2P, etc.	Yes	No	Available for many types of instruments	The substrates used in these procedures are not found in nature/medicine	[22, 27a, 28, 31, 33a, 35b, 36]
Detecting phosphate	Malachite Green, Molybdenum Blue	No	Yes	Effectively universal	Inconvenient and discontinuous	[43–45]
Detecting specific recognition	Supramolecular chemosensors, fluorescent probes, gold nanoparticles	Yes	No	Convenient and rapid procedures	Different assays are required for every type of substrate, and they are not available for all substrates	[53, 56, 60, 64–65, 69–70]
Detecting directly	IR, MS, NMR	Yes/No	Yes	Can confirm the identity of product molecules	Overlapping bands (IR), complex protocols (MS, NMR)	[73, 75, 76b, 77c, 80]
Detecting thermodynamics	ITC, IrCal	Yes	Yes	No labelling required and it works for any substrate	Less amenable to high-throughput screening	[81a, 82–83]
Detecting conformational change	Fluorescent nanoantennas	Yes	Yes	Rapid characterisation of any substrate in one shot	Biotin-streptavidin or other attachment chemistry is needed to drive dye-protein interaction	[91]

Table 2. Comparison of reported experimental conditions for methods to study AP enzyme with ATP as its substrate.

Method	[ATP] (μM)	[AP] (nM)	Reference
Fluorescent Probe	5 to 200	n/a[a]	[56]
Supramolecular Chemosensor	15 to 60	n/a[a]	[66]
IR	50000	n/a[a]	[73]
ESI-MS	40	44.64	[76b]
IrCal	0.5 to 21.4	3.7	[82]
Fluorescent Nanoantennas	300	20	[91]
Molybdenum Blue	5 to 60	n/a[a]	[97]
Malachite Green	10 to 700	1[b]	[94]

[a] These studies did not state the molar concentration of AP. [b] It is unclear if this concentration was used in all experiments in this study.

is several orders of magnitude greater than the enzyme concentrations and is close to reported K_M values.[56,66,82,91,94,97] We note that these methods are not limited to the concentrations listed in the table. For example, with fluorescent nanoantennas, we used these concentrations to study ATP, but also used various other enzyme and substrate concentrations elsewhere in the study.[91]

Despite numerous signal-generating substrates having been developed, recent works have continued to employ the classic substrates. For example, pNPP has been used to investigate TNAP mutations,[11] monofluorinated alkyl phosphates for food packaging materials,[76c] a chimeric AP with therapeutic potential,[94] inhibition,[97] macromolecular crowding,[98] and AP from a parasitic flatworm.[99] However, these studies investigated APs with biomolecular substrates too, some already mentioned herein (ATP, ADP, AMP, PLP, PP_i, and LPS), and others such as cytidine monophosphate (CMP), thymidine monophosphate (TMP), guanosine monophosphate (GMP), sphingosine-1-phosphate (S1P), and polyphosphate (PolyP). Characterising these substrates required the use of discontinuous P_i detection assays (e.g., malachite green assay). Similar situations have arisen in studies of acid phosphatases, too.[100] This observation highlights the importance of continuing to develop assays for convenient and rapid characterisation of biological and medicinal substrates of APs. Ideally, new assays will be universal for any substrate of this enzyme. In conclusion, we hope that these emerging and classic methods to study AP with natural and medicinal substrates discussed herein, and those to come, will find increased application in the coming years to help us learn more about this vital enzyme.

4. Note

The crystal structures in the frontispiece image represent cold-active *Vibrio* sp. alkaline phosphatase (turquoise, 3E2D),[101] *Escherichia coli* (*E. coli*) alkaline phosphatase (violet, 1ALK),[102] *Rattus norvegicus* (rat) intestinal alkaline phosphatase (red, 4KJG),[103] and human placental alkaline phosphatase (yellow, 1EW2).[104] 3D protein structures were drawn with UCSF ChimeraX software,[105] and molecular structures were drawn with MarvinSketch software (ChemAxon, Budapest, Hungary).

Acknowledgements

S. G. H. acknowledges a Banting Postdoctoral Fellowship and support from the TransMedTech Institute (Canada First Research Excellence Fund) as well as previous doctoral scholarships from the National Sciences and Engineering Research Council of Canada (NSERC) and Fonds de recherche du Québec – Nature et technologies (FRQNT). A. V. B. acknowledges support from NSERC, Canada Research Chairs, FRQNT, and Le regroupement québécois de recherche sur la fonction, l'ingénierie et les applications des protéines (PROTEO).

Conflict of Interests

The authors declare no conflict of interest.

Data Availability Statement

Data sharing is not applicable to this article as no new data were created or analyzed in this study.

Keywords: alkaline phosphatase · biosensors · enzyme assays · natural substrates · DNA nanotechnology

[1] a) H. Fu, J. Cao, T. Qiao, Y. Qi, S. J. Charnock, S. Garfinkle, T. K. Hyster, *Nature* **2022**, *610*, 302–307; b) N. J. Porter, E. Danelius, T. Gonen, F. H. Arnold, *J. Am. Chem. Soc.* **2022**, *144*, 8892–8896.
[2] X. Zhao, K. Gentile, F. Mohajerani, A. Sen, *Acc. Chem. Res.* **2018**, *51*, 2373–2381.
[3] M. P. Whyte, C. R. Greenberg, N. J. Salman, M. B. Bober, W. H. McAlister, D. Wenkert, B. J. Van Sickle, J. H. Simmons, T. S. Edgar, M. L. Bauer, M. A. Hamdan, N. Bishop, R. E. Lutz, M. McGinn, S. Craig, J. N. Moore, J. W. Taylor, R. H. Cleveland, W. R. Cranley, R. Lim, T. D. Thacher, J. E. Mayhew, M. Downs, J. L. Millán, A. M. Skrinar, P. Crine, H. Landy, *N. Engl. J. Med.* **2012**, *366*, 904–913.
[4] J. Chapman, A. E. Ismail, C. Z. Dinu, *Catalysts* **2018**, *8*, 238.
[5] A. F. Siller, M. P. Whyte, *J. Bone Miner. Res.* **2018**, *33*, 362–364.
[6] S. Sharifian, A. Homaei, S.-K. Kim, M. Satari, *Process Biochem.* **2018**, *64*, 103–115.
[7] J.-P. Lallès, *Fish Shellfish Immunol.* **2019**, *89*, 179–186.
[8] B. Le-Vinh, Z. B. Akkuş-Dağdeviren, N.-M. N. Le, I. Nazir, A. Bernkop-Schnürch, *Adv. Ther.* **2022**, *5*, 2100219.
[9] a) U. Sharma, D. Pal, R. Prasad, *Ind. J. Clin. Biochem.* **2014**, *29*, 269–278; b) M. Haarhaus, V. Brandenburg, K. Kalantar-Zadeh, P. Stenvinkel, P. Magnusson, *Nat. Rev. Nephrol.* **2017**, *13*, 429–442; c) M.-H. Le Du, J. L. Millán, *J. Biol. Chem.* **2002**, *277*, 49808–49814.
[10] B. A. Rader, *Front. Immunol.* **2017**, *8*, 897.
[11] S. Di Mauro, T. Manes, L. Hessle, A. Kozlenkov, J. M. Pizauro Jr., M. F. Hoylaerts, J. L. Millán, *J. Bone Miner. Res.* **2002**, *17*, 1383–1391.
[12] a) J. L. Millán, M. P. Whyte, *Calcif. Tissue Int.* **2016**, *98*, 398–416; b) C. Goettsch, A. Strzelecka-Kiliszek, L. Bessueille, T. Quillard, L. Mechtouff, S. Pikula, E. Canet-Soulas, M. J. Luis, C. Fonta, D. Magne, *Cardiovasc. Res.* **2020**, *118*, 84–96; c) C.-L. Bartlett, E. M. Cave, N. J. Crowther, W. F. Ferris, *Mol. Cell. Biochem.* **2022**, *477*, 2093–2106.
[13] L. Bessueille, L. Kawtharany, T. Quillard, C. Goettsch, A. Briolay, N. Taraconat, S. Balayssac, V. Gilard, S. Mebarek, O. Peyruchaud, F. Duboeuf, C. Bouillot, A. Pinkerton, L. Mechtouff, R. Buchet, E. Hamade, K. Zibara, C. Fonta, E. Canet-soulas, J. l. Millan, D. Magne, *Transl. Res.* **2023**.
[14] a) J. Fawley, D. M. Gourlay, *J. Surg. Res.* **2016**, *202*, 225–234; b) F. Kühn, R. Duan, M. Ilmer, U. Wirth, F. Adiliaghdam, T. S. Schiergens, J. Andrassy, A. V. Bazhin, J. Werner, *Visc. Med.* **2021**, *37*, 383–393; c) S. B. Singh, H. C. Lin, *Biomol. Eng.* **2021**, *11*, 1784; d) W. H. Yang, D. M. Heithoff, P. V. Aziz, M. Sperandio, V. Nizet, M. J. Mahan, J. D. Marth, *Science* **2017**, *358*, eaao5610.
[15] a) M. King, S. Joseph, A. Albert, T. V. Thomas, M. R. Nittala, W. C. Woods, S. Vijayakumar, S. Packianathan, *Oncology* **2020**, *98*, 61–80; b) J. Rautio, N. A. Meanwell, L. Di, M. J. Hageman, *Nat. Rev. Drug Discovery* **2018**, *17*, 559–587; c) A. Newland, V. McDonald, *Immunotherapy* **2020**, *12*, 1325–1340; d) C. L. Pervan-Steel, U. Roy Chowdhury, H. K. Sookdeo, R. A. Casale, P. I. Dosa, T. M. Htoo, M. P. Fautsch, B. M. Wirostko, *Invest. Ophthalmol. Visual Sci.* **2022**, *63*, 26–26; e) R. J. Dinis-Oliveira, *Drug Metab. Rev.* **2017**, *49*, 84–91; f) H. Yu, H. Yang, E. Shi, W. Tang, *Med. Drug Discov.* **2020**, *8*, 100063.
[16] a) P. J. Skelly, C. S. Nation, A. A. Da'Dara, *Trends Parasitol.* **2022**, *38*, 1080–1088; b) E. Xie, Y. Su, S. Deng, M. Kontopyrgou, D. Zhang, *Environ. Pollut.* **2021**, *268*, 115807; c) Q. Liu, A. J. Parsons, H. Xue, C. S. Jones, S. Rasmussen, *Fungal Genet. Biol.* **2013**, *54*, 52–59; d) D.-H. Lee, S.-L. Choi, E. Rha, S. J. Kim, S.-J. Yeom, J.-H. Moon, S.-G. Lee, *BMC Biotechnol.* **2015**, *15*, 1; e) K. Zhang, J. Li, J. Wang, X. Lin, L. Li, Y. You, X. Wu, Z. Zhou, S. Lin, *Mol. Ecol.* **2022**, *31*, 3389–3399.
[17] a) M. Dasnur Nanjappa, A. Pandith, S. Sankaran, D. P. Dorairaj, A. A. Reddy, H. P. B. Ramesh, *Symmetry* **2022**, *14*, 1634; b) S. M. Shaban, S. Byeok Jo, E. Hafez, J. Ho Cho, D.-H. Kim, *Coord. Chem. Rev.* **2022**, *465*, 214567.
[18] O. A. Bessey, O. H. Lowry, M. J. Brock, *J. Biol. Chem.* **1946**, *164*, 321–329.
[19] S. Markússon, J. G. Hjörleifsson, P. Kursula, B. Ásgeirsson, *Biochemistry* **2022**, *61*, 2248–2260.
[20] A. Srivastava, D. E. M. Saavedra, B. Thomson, J. A. L. García, Z. Zhao, W. M. Patrick, G. J. Herndl, F. Baltar, *ISME J.* **2021**, *15*, 3375–3383.
[21] H. Fernley, P. Walker, *Biochem. J.* **1965**, *97*, 95–103.
[22] Y. Jiang, X. Li, D. R. Walt, *Angew. Chem. Int. Ed.* **2020**, *59*, 18010–18015; *Angew. Chem.* **2020**, *132*, 18166–18171.
[23] V. B. Paragas, Y.-Z. Zhang, R. P. Haugland, V. L. Singer, *J. Histochem. Cytochem.* **1997**, *45*, 345–357.
[24] a) A. K. Ghosh, V. L. Schramm, *Biochemistry* **2021**, *60*, 118–124; b) A. Nukazuka, S. Asai, K. Hayakawa, K. Nakagawa, M. Kanazashi, H. Kakizoe, K. Hayashi, T. Kawahara, K. Sawada, H. Kuno, K. Kano, *Sens. Bio-Sens. Res.* **2023**, *39*, 100549.
[25] J. Liang, R. T. K. Kwok, H. Shi, B. Z. Tang, B. Liu, *ACS Appl. Mater. Interfaces* **2013**, *5*, 8784–8789.
[26] M. Tian, K. Zhang, Y. Zhang, H. Zhou, Z. Yuan, C. Lu, *Anal. Chim. Acta* **2021**, *1143*, 144–156.
[27] a) L. Gwynne, A. C. Sedgwick, J. E. Gardiner, G. T. Williams, G. Kim, J. P. Lowe, J.-Y. Maillard, A. T. A. Jenkins, S. D. Bull, J. L. Sessler, J. Yoon, T. D. James, *Front. Chem.* **2019**, *7*; b) X. Jie, M. Wu, H. Yang, W. Wei, *Anal. Chem.* **2019**, *91*, 13174–13182; c) X. Pang, Y. Li, Q. Lu, Z. Ni, Z. Zhou, R. Xie, C. Wu, H. Li, Y. Zhang, *Analyst* **2021**, *146*, 521–528; d) Y. Tan, L. Zhang, K. H. Man, R. Peltier, G. Chen, H. Zhang, L. Zhou, F. Wang, D. Ho, S. Q. Yao, Y. Hu, H. Sun, *ACS Appl. Mater. Interfaces* **2017**, *9*, 6796–6803; e) S.-J. Li, C.-Y. Li, Y.-F. Li, J. Fei, P. Wu, B. Yang, J. Ou-Yang, S.-X. Nie, *Anal. Chem.* **2017**, *89*, 6854–6860.
[28] H.-W. Liu, K. Li, X.-X. Hu, L. Zhu, Q. Rong, Y. Liu, X.-B. Zhang, J. Hasserodt, F.-L. Qu, W. Tan, *Angew. Chem. Int. Ed.* **2017**, *56*, 11788–11792; *Angew. Chem.* **2017**, *129*, 11950–11954.
[29] H. He, J. Guo, J. Xu, J. Wang, S. Liu, B. Xu, *Nano Lett.* **2021**, *21*, 4078–4085.
[30] a) H. Zhang, P. Xiao, Y. T. Wong, W. Shen, M. Chhabra, R. Peltier, Y. Jiang, Y. He, J. He, Y. Tan, Y. Xie, D. Ho, Y.-W. Lam, J. Sun, H. Sun, *Biomaterials* **2017**, *140*, 220–229; b) Y. Jia, P. Li, K. Han, *Chem. Asian J.* **2015**, *10*, 2444–2451.
[31] S. Sakamoto, T. Komatsu, R. Watanabe, Y. Zhang, T. Inoue, M. Kawaguchi, H. Nakagawa, T. Ueno, T. Okusaka, K. Honda, H. Noji, Y. Urano, *Sci. Adv.* **2020**, *6*, eaay0888.
[32] Y. Yang, M. Zhang, W. Zhang, Y. Chen, T. Zhang, S. Chen, Y. Yuan, G. Liang, S. Zhang, *Analyst* **2022**, *147*, 1544–1550.
[33] a) S. Goggins, C. Naz, B. J. Marsh, C. G. Frost, *Chem. Commun.* **2015**, *51*, 561–564; b) T. Balbaied, A. Hogan, E. Moore, *Biosensors* **2020**, *10*, 95; c) M. Bekhit, T. Blazek, W. Gorski, *Anal. Chem.* **2021**, *93*, 14280–14286.
[34] C. Pezzato, J. L. Y. Chen, P. Galzerano, M. Salvi, L. J. Prins, *Org. Biomol. Chem.* **2016**, *14*, 6811–6820.
[35] a) C. Ruan, W. Wang, B. Gu, *Anal. Chem.* **2006**, *78*, 3379–3384; b) D. Sun, W. Xu, C. Liang, W. Shi, S. Xu, *ACS Sens.* **2020**, *5*, 1758–1767; c) D. Sun, W. Xu, S. Xu, *Anal. Methods* **2019**, *11*, 3501–3505; d) A. Ingram, B. D. Moore, D. Graham, *Bioorg. Med. Chem. Lett.* **2009**, *19*, 1569–1571.
[36] I. Daryaei, M. Mohammadebrahim Ghaffari, K. M. Jones, M. D. Pagel, *ACS Sens.* **2016**, *1*, 857–861.
[37] U. Sanzhaeva, X. Xu, P. Guggilapu, M. Tseytlin, V. V. Khramtsov, B. Driesschaert, *Angew. Chem. Int. Ed.* **2018**, *57*, 11701–11705; *Angew. Chem.* **2018**, *130*, 11875–11879.
[38] K. Tanaka, N. Kitamura, Y. Chujo, *Bioconjugate Chem.* **2011**, *22*, 1484–1490.
[39] T. Kuwahara, T. Homma, M. Kondo, M. Shimomura, *Biosens. Bioelectron.* **2011**, *26*, 3382–3385.
[40] N. Nagy, H. F. Kuipers, A. R. Frymoyer, H. D. Ishak, J. B. Bollyky, T. N. Wight, P. L. Bollyky, *Front. Immunol.* **2015**, *6*.
[41] A. Pabis, S. C. L. Kamerlin, *Curr. Opin. Struct. Biol.* **2016**, *37*, 14–21.
[42] A. A. Recoulat Angelini, S. A. Martínez Gache, M. L. Sabeckis, N. A. Melian, F. L. González Flecha, *New J. Chem.* **2022**, *46*, 12401–12409.
[43] S. A. Martínez Gache, A. A. Recoulat Angelini, M. L. Sabeckis, F. L. González Flecha, *Anal. Biochem.* **2020**, *597*, 113681.
[44] E. A. Nagul, I. D. McKelvie, P. Worsfold, S. D. Kolev, *Anal. Chim. Acta* **2015**, *890*, 60–82.
[45] A. A. Baykov, O. A. Evtushenko, S. M. Avaeva, *Anal. Biochem.* **1988**, *171*, 266–270.
[46] J. Feng, Y. Chen, J. Pu, X. Yang, C. Zhang, S. Zhu, Y. Zhao, Y. Yuan, H. Yuan, F. Liao, *Anal. Biochem.* **2011**, *409*, 144–149.
[47] M. R. Webb, *Proc. Natl. Acad. Sci. USA* **1992**, *89*, 4884–4887.
[48] M. Brune, J. L. Hunter, J. E. T. Corrie, M. R. Webb, *Biochemistry* **1994**, *33*, 8262–8271.
[49] M. N. Levine, R. T. Raines, *Anal. Biochem.* **2011**, *418*, 247–252.
[50] P. Schrenkhammer, I. C. Rosnizeck, A. Duerkop, O. S. Wolfbeis, M. Schäferling, *J. Biomol. Screening* **2008**, *13*, 9–16.

[51] a) Z. Qian, L. Chai, C. Tang, Y. Huang, J. Chen, H. Feng, *Anal. Chem.* **2015**, *87*, 2966–2973; b) L. Chen, G. Yang, P. Wu, C. Cai, *Biosens. Bioelectron.* **2017**, *96*, 294–299; c) C. Chen, J. Zhao, Y. Lu, J. Sun, X. Yang, *Anal. Chem.* **2018**, *90*, 3505–3511.
[52] H. Li, Y. Sun, Y. Li, J. Du, *Microchem. J.* **2021**, *160*, 105665.
[53] Y. Liu, K. S. Schanze, *Anal. Chem.* **2008**, *80*, 8605–8612.
[54] P. Raj, A. Singh, A. Singh, A. Singh, N. Garg, N. Kaur, N. Singh, *Eur. J. Inorg. Chem.* **2019**, *2019*, 628–638.
[55] Z. S. Qian, L. J. Chai, Y. Y. Huang, C. Tang, J. Jia Shen, J. R. Chen, H. Feng, *Biosens. Bioelectron.* **2015**, *68*, 675–680.
[56] J. Chen, H. Jiao, W. Li, D. Liao, H. Zhou, C. Yu, *Chem. Asian J.* **2013**, *8*, 276–281.
[57] P. Rana, A. Jennifer, G. M. Siva, E. Varathan, P. Das, *New J. Chem.* **2022**, *46*, 23139–23154.
[58] R. Nutiu, J. M. Y. Yu, Y. Li, *ChemBioChem* **2004**, *5*, 1139–1144.
[59] W. Zhao, W. Chiuman, J. C. F. Lam, M. A. Brook, Y. Li, *Chem. Commun.* **2007**, 3729–3731.
[60] F. Lu, M.-J. Wu, C.-J. Yu, X. Gao, H. Zhou, Z. Yuan, *Sens. Actuators B* **2020**, *325*, 128959.
[61] C. Chen, D. Zhao, Y. Jiang, P. Ni, C. Zhang, B. Wang, F. Yang, Y. Lu, J. Sun, *Anal. Chem.* **2019**, *91*, 15017–15024.
[62] A. Hennig, H. Bakirci, W. M. Nau, *Nat. Methods* **2007**, *4*, 629–632.
[63] R. N. Dsouza, A. Hennig, W. M. Nau, *Chem. Eur. J.* **2012**, *18*, 3444–3459.
[64] Y.-C. Liu, S. Peng, L. Angelova, W. M. Nau, A. Hennig, *ChemistryOpen* **2019**, *8*, 1350–1354.
[65] Y. Liu, J. Lee, L. Perez, A. D. Gill, R. J. Hooley, W. Zhong, *J. Am. Chem. Soc.* **2018**, *140*, 13869–13877.
[66] K. Wang, J.-H. Cui, S.-Y. Xing, H.-X. Dou, *Org. Biomol. Chem.* **2016**, *14*, 2684–2690.
[67] Y.-X. Yue, Y. Kong, F. Yang, Z. Zheng, X.-Y. Hu, D.-S. Guo, *ChemistryOpen* **2019**, *8*, 1437–1440.
[68] S. Sinn, F. Biedermann, *Isr. J. Chem.* **2018**, *58*, 357–412.
[69] F. Biedermann, D. Hathazi, W. M. Nau, *Chem. Commun.* **2015**, *51*, 4977–4980.
[70] F. Biedermann, G. Ghale, A. Hennig, W. M. Nau, *Commun. Biol.* **2020**, *3*, 383.
[71] N. M. Kumar, P. Picchetti, C. Hu, L. M. Grimm, F. Biedermann, *ACS Sens.* **2022**, *7*, 2312–2319.
[72] a) L. Zhang, R. Buchet, G. Azzar, *Biophys. J.* **2004**, *86*, 3873–3881; b) L. Zhang, R. Buchet, G. Azzar, *Biochem. Biophys. Res. Commun.* **2005**, *328*, 591–594.
[73] Z. Ren, L. D. Do, G. Bechkoff, S. Mebarek, N. Keloglu, S. Ahamada, S. Meena, D. Magne, S. Pikula, Y. Wu, R. Buchet, *PLoS One* **2015**, *10*, e0120087.
[74] Z. Ren, L. Zhang, Y. Wu, S. Mebarek, R. Buchet, *Vib. Spectrosc.* **2016**, *86*, 206–211.
[75] R. Buchet, C. Tribes, V. Rouaix, B. Doumèche, M. Fiore, Y. Wu, D. Magne, S. Mebarek, *Int. J. Mol. Sci.* **2021**, *22*, 2948.
[76] a) T. Burkhardt, C. M. Kaufmann, T. Letzel, J. Grassmann, *ChemBioChem* **2015**, *16*, 1985–1992; b) C. M. Kaufmann, J. Graßmann, D. Treutter, T. Letzel, *Rapid Commun. Mass Spectrom.* **2014**, *28*, 869–878; c) D. A. Jackson, S. A. Mabury, *Environ. Toxicol. Chem.* **2012**, *31*, 1966–1971.
[77] a) H. Yuan, N. Li, Y. Lai, *Drug Metab. Dispos.* **2009**, *37*, 1443–1447; b) Y. Wang, Y. Li, J. Lu, H. Qi, I. Cheng, H. Zhang, *Molecules* **2018**, *23*, 1195; c) H. O'Dowd, D. E. Shannon, K. R. Chandupatla, V. Dixit, J. J. Engtrakul, Z. Ye, S. M. Jones, C. F. O'Brien, D. P. Nicolau, P. R. Tessier, J. L. Crandon, B. Song, D. Macikenas, B. L. Hanzelka, A. Le Tiran, Y. L. Bennani, P. S. Charifson, A.-L. Grillot, *ACS Med. Chem. Lett.* **2015**, *6*, 822–826.
[78] H. Yamaguchi, M. Zaima, M. Adachi, Y. Tomaru, H. Asahara, N. Nishiwaki, *Phycological Res.* **2022**, *70*, 151–159.
[79] B. Wan, R. Huang, J. M. Diaz, Y. Tang, *Sci. Total Environ.* **2022**, *833*, 155187.
[80] J. Pinkston, R. Shen, C. R. Simons, A. C. Hengge, *Anal. Biochem.* **2022**, *651*, 114727.
[81] a) Y. Wang, G. Wang, N. Moitessier, A. K. Mittermaier, *Front. Mol. Biosci.* **2020**, *7*; b) P.-L. Hagedoorn, *Front. Catal.* **2022**, *2*; c) M. J. Todd, J. Gomez, *Anal. Biochem.* **2001**, *296*, 179–187; d) M. K. Transtrum, L. D. Hansen, C. Quinn, *Methods* **2015**, *76*, 194–200.
[82] K. Honarmand Ebrahimi, P.-L. Hagedoorn, D. Jacobs, W. R. Hagen, *Sci. Rep.* **2015**, *5*, 16380.
[83] J. M. Di Trani, N. Moitessier, A. K. Mittermaier, *Anal. Chem.* **2017**, *89*, 7022–7030.
[84] J. M. Di Trani, N. Moitessier, A. K. Mittermaier, *Anal. Chem.* **2018**, *90*, 8430–8435.
[85] M. M. C. H. van Schie, K. H. Ebrahimi, W. R. Hagen, P.-L. Hagedoorn, *Anal. Biochem.* **2018**, *544*, 57–63.
[86] R. Zhou, O. Yang, A.-C. Déclais, H. Jin, G. H. Gwon, A. D. J. Freeman, Y. Cho, D. M. J. Lilley, T. Ha, *Nat. Chem. Biol.* **2019**, *15*, 269–275.
[87] a) C.-Y. Lee, C. McNerney, K. Ma, W. Zhao, A. Wang, S. Myong, *Nat. Commun.* **2020**, *11*, 3392; b) F. Rashid, V.-S. Raducanu, M. S. Zaher, M. Tehseen, S. Habuchi, S. M. Hamdan, *Nat. Commun.* **2019**, *10*, 2104; c) L. D. F. Nielsen, M. Hansen-Bruhn, M. A. D. Nijenhuis, K. V. Gothelf, *ACS Sens.* **2022**, *7*, 856–865.
[88] H.-W. Au, M.-W. Tsang, P.-K. So, K.-Y. Wong, Y.-C. Leung, *ACS Omega* **2019**, *4*, 20493–20502.
[89] a) C. Hu, L. Grimm, A. Prabodh, A. Baksi, A. Siennicka, P. A. Levkin, M. M. Kappes, F. Biedermann, *Chem. Sci.* **2020**, *11*, 11142–11153; b) R. Griss, A. Schena, L. Reymond, L. Patiny, D. Werner, C. E. Tinberg, D. Baker, K. Johnsson, *Nat. Chem. Biol.* **2014**, *10*, 598–603.
[90] a) S. G. Harroun, C. Prévost-Tremblay, D. Lauzon, A. Desrosiers, X. Wang, L. Pedro, A. Vallée-Bélisle, *Nanoscale* **2018**, *10*, 4607–4641; b) E. Del Grosso, A.-M. Dallaire, A. Vallée-Bélisle, F. Ricci, *Nano Lett.* **2015**, *15*, 8407–8411.
[91] S. G. Harroun, D. Lauzon, M. C. C. J. C. Ebert, A. Desrosiers, X. Wang, A. Vallée-Bélisle, *Nat. Methods* **2022**, *19*, 71–80.
[92] Y. T. Tamer, I. K. Gaszek, H. Abdizadeh, T. A. Batur, K. A. Reynolds, A. R. Atilgan, C. Atilgan, E. Toprak, *Mol. Biol. Evol.* **2019**, *36*, 1533–1550.
[93] A. Iyer, A. Chandra, R. Swaminathan, *Biochim. Biophys. Acta Gen. Subj.* **2014**, *1840*, 2935–2943.
[94] T. Kiffer-Moreira, C. R. Sheen, K. C. d. S. Gasque, M. Bolean, P. Ciancaglini, A. van Elsas, M. F. Hoylaerts, J. L. Millán, *PLoS One* **2014**, *9*, e89374.
[95] A. Mumtaz, K. Saeed, A. Mahmood, S. Zaib, A. Saeed, J. Pelletier, J. Sévigny, J. Iqbal, *Bioorg. Chem.* **2020**, *101*, 103996.
[96] a) G. L. Borosky, *J. Chem. Inf. Model.* **2020**, *60*, 6228–6241; b) G. L. Borosky, *J. Chem. Inf. Model.* **2017**, *57*, 540–549.
[97] G. Katsipis, V. Tsalouxidou, E. Halevas, E. Geromichalou, G. Geromichalos, A. A. Pantazaki, *Appl. Microbiol. Biotechnol.* **2021**, *105*, 147–168.
[98] A. Deshwal, S. Maiti, *Langmuir* **2021**, *37*, 7273–7284.
[99] a) M. Elzoheiry, A. A. Da'dara, R. Bhardwaj, Q. Wang, M. S. Azab, E.-S. I. El-Kholy, S. N. El-Beshbishi, P. J. Skelly, *Front. Immunol.* **2018**, *9*; b) M. Elzoheiry, A. A. Da'dara, C. S. Nation, S. N. El-Beshbishi, P. J. Skelly, *Mol. Biochem. Parasitol.* **2019**, *232*, 111190; c) A. A. Da'dara, M. Elzoheiry, S. N. El-Beshbishi, P. J. Skelly, *Front. Immunol.* **2021**, *11*, 622162.
[100] a) S. S. Rangu, R. Singh, N. K. Gaur, D. Rath, R. D. Makde, R. Mukhopadhyaya, *Biotechnol. Rep.* **2022**, *33*, e00709; b) S. Deng, J. Li, Z. Du, Z. Wu, J. Yang, H. Cai, G. Wu, F. Xu, Y. Huang, S. Wang, C. Wang, *Plant Cell Environ.* **2022**, *45*, 191–205.
[101] R. Helland, R. L. Larsen, B. Ásgeirsson, *Biochim. Biophys. Acta Proteins Proteomics* **2009**, *1794*, 297–308.
[102] E. E. Kim, H. W. Wyckoff, *J. Mol. Biol.* **1991**, *218*, 449–464.
[103] K. Ghosh, D. Mazumder Tagore, R. Anumula, B. Lakshmaiah, P. P. B. S. Kumar, S. Singaram, T. Matan, S. Kallipatti, S. Selvam, P. Krishnamurthy, M. Ramarao, *J. Struct. Biol.* **2013**, *184*, 182–192.
[104] M. H. Le Du, T. Stigbrand, M. J. Taussig, A. Ménez, E. A. Stura, *J. Biol. Chem.* **2001**, *276*, 9158–9165.
[105] E. F. Pettersen, T. D. Goddard, C. C. Huang, E. C. Meng, G. S. Couch, T. I. Croll, J. H. Morris, T. E. Ferrin, *Protein Sci.* **2021**, *30*, 70–82.
[106] E. B. Cogan, G. B. Birrell, O. H. Griffith, *Anal. Biochem.* **1999**, *271*, 29–35.

Manuscript received: November 22, 2022
Version of record online: ■■, ■■■

REVIEW

Alkaline phosphatase kinetics measurements are easy to follow with non-natural chromogenic and fluorogenic substrates, but less so with biological and medicinal substrates. This review discusses the recent and key methods that one can employ to characterise this enzyme's kinetics, with an emphasis on spectroscopically silent biomolecular substrates. The principles described herein ought to apply to other enzyme-substrate systems too.

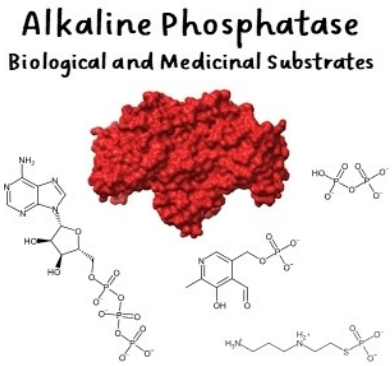

Dr. S. G. Harroun, Prof. Dr. A. Vallée-Bélisle**

1 – 14

Methods to Characterise Enzyme Kinetics with Biological and Medicinal Substrates: The Case of Alkaline Phosphatase